

Elemental mixing systematics and Sr–Nd isotope geochemistry of mélangé formation: Obstacles to identification of fluid sources to arc volcanics

Robert L. King^{a,b,*}, Gray E. Bebout^{a,b}, Takuya Moriguti^b, Eizo Nakamura^b

^a Department of Earth and Environmental Sciences, Lehigh University, 31 Williams Drive, Bethlehem, PA 18015, USA

^b The Pheasant Memorial Laboratory for Geochemistry and Cosmochemistry, Institute for Study of the Earth's Interior, Okayama University at Misasa, Tottori-ken, 682-0193, Japan

Received 27 June 2005; received in revised form 17 March 2006; accepted 29 March 2006

Available online 24 May 2006

Editor: K. Farley

Abstract

We present major and trace element concentrations in conjunction with Sr–Nd isotope ratios to investigate the geochemical characteristics of mélangé formation along the subduction zone slab–mantle interface. Mélangé matrix of the Catalina Schist formed within an active subduction zone of the southern California borderland in Cretaceous time. Mélangé formed through the synergistic effects of deformation and metasomatic fluid flow affecting peridotite, basaltic, and sedimentary protoliths to form hybridized bulk compositions not typical of seafloor “input” lithologies. In general, all elemental concentrations primarily reflect mechanical mixing processes, while fluid flow mediates all elemental systematics to a varying extent that is largely a function of inferred “mobility” for a particular element or the stability of suitable mineral hosts. Elemental data reveal that mineral stabilities defined by the evolution of bulk composition within mélangé zones are probably the most important control of solid, liquid, or fluid geochemistry within the subduction system. Sr–Nd isotope ratios are highly variable and reflect contributions of mélangé protoliths to varying extents. A weak mechanical mixing array present in Sr isotope data is strongly overprinted by a fluid signal that dominates mélangé Sr systematics. Nd isotope data suggest that Nd is more conservative during metamorphism and is largely controlled by mechanical mixing. We argue that mélangé formation is an intrinsic process to all subduction zones and that the geochemistry of mélangé will impart the strongest control on the geochemistry of metasomatic agents (hydrous fluids, silicate melts, or miscible supercritical liquids) progressing to arc magmatic source regions in the mantle wedge. Mélangé formation processes suggest that comparisons of subduction “inputs” to arc volcanic “outputs” as a means to infer recycling at subduction zones dangerously over-simplify the physics of the mass transfer in subduction zones, as subducted mass is consistently redistributed into novel bulk compositions. Such mélangé zones along the slab–mantle interface simultaneously bear characteristic elemental or isotopic signals of several distinct input lithologies, while experiencing phase equilibria not typical of any input. We recommend that future studies explore the phase equilibria of hybridized systems and mineral trace element residency, as these processes provide for a physical baseline from which it will be possible to follow the path of subducted mass through the system. © 2006 Elsevier B.V. All rights reserved.

Keywords: subduction zones; metamorphic; petrology; mélangé; geochemistry; isotope geochemistry

* Corresponding author. Department of Earth and Environmental Sciences, Lehigh University, 31 Williams Drive, Bethlehem, PA 18015, USA.
E-mail address: robbie@lehigh.edu (R.L. King).

1. Introduction

Analyses of arc volcanic rocks have long recognized the importance of metamorphic reactions and processes to arc magmatic petrogenesis and recycling to the mantle. However, despite igneous constraints, linking exact metamorphic processes to the development of distinct magmatic geochemical compositions has been ambiguous, especially since the geochemistry of metamorphic rocks beneath arcs is a combination of conjecture based on pre-subduction seafloor compositions (i.e. [1–3]) and the comparatively limited data for subduction-zone metamorphic rocks [4–13]. Even more problematic is that data do not exist for the entire metamorphic suite produced within subduction zones, so our appreciation of the full spectrum of petrologic processes and their geochemical effects is incomplete. Most conspicuous among the missing data is a description of the geochemical ramifications of *mélange* formation.

Tectonic *mélange* is one of the most characteristic by-products of the subduction cycle, occurring in most orogenic belts. Styles and petrologic settings of *mélange* can range from highly deformed metasedimentary collages typical of incipient metamorphism within accretionary prisms (e.g. [14]) to chaotic hybridized mixtures of peridotite, basalt, and sediment produced at blueschist-, amphibolite-, or eclogite-facies conditions in forearc to sub-arc regions (e.g. [5–7,15]). In all instances, *mélange* formation appears intimately linked to reactive fluid flow, indicating metasomatic processes are important in addition to mechanical deformation.

The extent and volumetric significance of *mélange* formation within deeper portions of subduction zones are debated, although anomalous geophysical results indicating deep subduction of hydrated material can be interpreted as measurement of *mélange*. Abers [16] reported seismic evidence for 1–7 km thick zones of anomalously slow material, interpreted by Abers [16] as hydrated oceanic crust along the surface of the subducting slab, in subduction zones worldwide. An intriguing alternative interpretation is that these seismically slow waveguides represent hydrated *mélange* zones dominated by chlorite + talc [7], a high-variance assemblage that will persist to the appropriate ~ 250 km depths [4,17]. This alternative interpretation suggests the possibility that *mélange* is an intrinsic feature of the slab–mantle interface and may play an important role in buffering fluid or melt compositions ultimately transferred to arc magma source regions in the mantle wedge.

Here, we explore the petrologic and geochemical diversity of *mélange* formed during active subduction in the Catalina Schist subduction complex exposed on Santa

Catalina Island, CA. We report major element, trace element, and Sr–Nd isotope geochemistry for a large number of *mélange* samples spanning ranges in bulk composition and metamorphic grade. Our current dataset expands upon the more limited dataset of Bebout and Barton [7] for the Catalina Schist amphibolite-facies *mélange* by including a samples recording lawsonite–albite and lawsonite blueschist metamorphic conditions reminiscent of existing models for subduction-zone geothermal gradients. The focus of the current contribution is an investigation of geochemical effects stemming from *mélange* formation, as opposed to the petrogenetic modeling of Bebout and Barton [7].

2. Samples and analytical methods

The Catalina Schist has well-documented ranges in both bulk composition and metamorphic grade [4–7,18,19]. Due to these factors and the expected variability stemming from *mélange* formation, we comprehensively analyzed a large population of *mélange* matrix samples formed at three metamorphic grades for major and trace elements ($n=58$), while a representative subset were analyzed for Sr–Nd isotope ratios ($n=29$). Samples of *mélange* were collected from zones of lawsonite–albite facies conditions of 150–250 °C, 0.3–0.7 GPa (herein referred to as “LA *mélange*”; total $n=16$, isotope $n=5$), lawsonite–blueschist facies conditions of 200–350 °C, 0.7–1.0 GPa (“LB *mélange*”; total $n=23$, isotope $n=11$), and amphibolite facies conditions of 600–700 °C, 0.9–1.3 GPa (“AM *mélange*”; total $n=19$, isotope $n=13$; see [18] for a summary tectonometamorphic evolution of the Catalina Schist). In all instances, metamorphic conditions experienced by *mélange* are based upon the petrology of nearby coherent blocks that contain diagnostic mineral assemblages. It is important to note that blocks in *mélange* and *mélange* matrix of the Catalina Schist described here are co-facial and share a common metamorphic history, as *mélange* matrix has developed directly from coherent blocks; this situation contrasts common occurrences of exotic blocks in *mélange* from subduction complexes such as the Franciscan Complex, where blocks commonly experience a metamorphic evolution unrelated to their matrix host. Furthermore, it is also important to note that *mélange* matrix of the Catalina Schist is present throughout the complex, and is as abundant as coherent lithologies within the system (see [7] for *mélange* mapped at the kilometer scale) and is, therefore, a significant proportion of the island and, by inference, subduction complexes of active subduction zones. This volumetric scale of the *mélange* zones is very similar to the scale of altered oceanic crust and sea-floor

sediment present within subducting lithosphere. The Catalina mélange matrix samples encompass a wide spectrum of mineralogy and geochemical composition, discussed in detail below.

A common objection to research bearing on the Catalina Schist is that the amphibolite unit represents pressure–temperature conditions not typical of inferred geothermal gradients typical of subduction zones. While this is a valid argument, it is important to recognize that the amphibolite unit appears to represent an important portion of the development of the subduction complex [18] and that the Mg-rich, high-variance mineralogy of the amphibolite mélange matrix (i.e., chlorite + talc ± ortho- and clin amphiboles) is not sensitive to increased pressures. Therefore, this assemblage is directly analogous to the type of mélange that likely extends to subarc depths [4,7,17]. In this regard, the amphibolite mélange matrix is a valuable proxy for the slab–mantle interface. The lower-grade units analyzed in this contribution record metamorphic conditions directly comparable to model predictions for subduction-zone geothermal conditions.

All geochemical analyses presented in this study were performed at the Pheasant Memorial Laboratory, Institute for Study of the Earth's Interior, Okayama University at Misasa, Japan (see online dataset). Major element, Cr and Ni concentrations were determined using X-ray fluorescence (XRF) with the full standard suite of the Japanese Geological Survey. 500 mg of sample was mixed with 5 g of lithium tetraborate flux to produce homogeneous glass disks, and all samples were analyzed in duplicate (errors were $\leq 1\%$, relative standard deviation). Analytical conditions were similar to those described by Takei [20] for this instrument.

Trace element concentrations were measured using inductively coupled plasma mass spectrometry (ICPMS). Every sample was duplicated, many samples were analyzed in triplicate, and agreement between replicate analyses was excellent (errors were $\leq 2\text{--}3\%$, relative standard deviation). Analysis of Li, Rb, Sr, Y, the rare-earth elements (REE), Cs, Ba, Pb, Th, and U was performed using ~ 100 mg sample sizes and concentrated HF–HClO₄ digestions; fluoride residues produced by the initial acid attack were removed by repeated re-dissolution in HClO₄ [21]. Final solutions were prepared as 0.5 M HNO₃, from which all elements were analyzed by a calibration curve method [22] except Li, which was determined by isotope dilution [23]. Analysis of B, Zr, Nb, Hf, and Ta followed a concentrated HF digestion, final solutions as 0.5 M HF, and measurement by isotope dilution for B, Zr, and Hf, and by calibration curve for Nb and Ta [24–26]. A majority of digestions for both me-

thods were performed in sealed Teflon bombs at 205 °C to digest resistant phases, while a minority of samples lacking resistant phases were digested using Teflon beakers. Chemistry to prepare final solutions following bomb digestion was identical in detail to the Teflon beaker methods.

Sr and Nd isotope ratios were measured using thermal ionization mass spectrometry (TIMS). The instrument used was a Finnigan MAT-262 TIMS. Sr and Nd solutions were prepared identically to the ICPMS method. Procedures for chromatographic separation and mass spectrometry for Sr [27] and Nd [28] are described elsewhere. The average ⁸⁷Sr/⁸⁶Sr measured value for the NIST 987 Sr isotope standard over the course of the study was 0.710202 (± 0.000016 , 2σ , $n=22$). Measured ¹⁴³Nd/¹⁴⁴Nd ratios were corrected using the averaged value of the La Jolla ¹⁴³Nd/¹⁴⁴Nd ratio measured over the course of this study (0.511866 \pm 0.000025; 2σ , $n=17$). Total procedural blanks for digestion and column chemistry were 40–60 pg for Sr and 2–5 pg for Nd; samples sizes were sufficiently large so that blanks were negligible and blank corrections were unnecessary.

3. Phenomenological model of mélange formation

Previous studies of the Catalina Schist have developed a model to explain the formation of mélange via the synergistic effects of fluid flow, metamorphism, and deformation occurring amongst the more “coherent” sedimentary, basaltic, and ultramafic blocks in the subduction complex; we briefly review this model here. Within the Catalina Schist, abundant subduction related fluid flow is evident, with the greatest extents of fluid–rock interaction and stable isotope homogenization occurring along zones of structural weakness, such as mélange zones and fractures [4–7]. This reactive fluid flow was the primary driving force in mélange development, as fluids hydrated and metasomatically altered sediments, basalts, and peridotites within the subduction complex [5–7,19]. These metasomatic reactions dramatically affect the rheology of the material (e.g. [29–31]), where minerals such as talc, chlorite, and amphiboles form metasomatic “rinds” replacing olivine, pyroxenes, and plagioclase of less “digested” core material. This important change to minerals that more readily deform via ductile deformation mechanisms results in a focusing of deformation along these metasomatic reaction zones and the continual stripping of rinds into highly deformed shear zones. As this process continues, these shear zones evolve through the progressive coalescence and aggradation of deformed rind material to large-scale zones of mélange, while tectonic blocks in mélange are formed as

large coherent tracts of basalt, sediment, or peridotite are concurrently reduced in size by metasomatic digestion and mechanically broken down by processes such as boudinage that are favored by contrasts in material strength. Mélange zones also incorporate other transient petrologic processes during deformation, such as incorporation of veins or melts into the evolving matrix [6]. Resulting exposures of *mélange* are highly deformed and

record block digestion and mixing of rind material at scales from a single outcrop (Fig. 1) to the kilometer scale (see [7] for *mélange* at the map scale). Mineralogy of *mélange* zones is highly affected by local block composition(s), but is also influenced by fluid-related metasomatic vectors (Table 1).

Due to this model for *mélange* formation, we provide a reference frame comparing compositional fields for

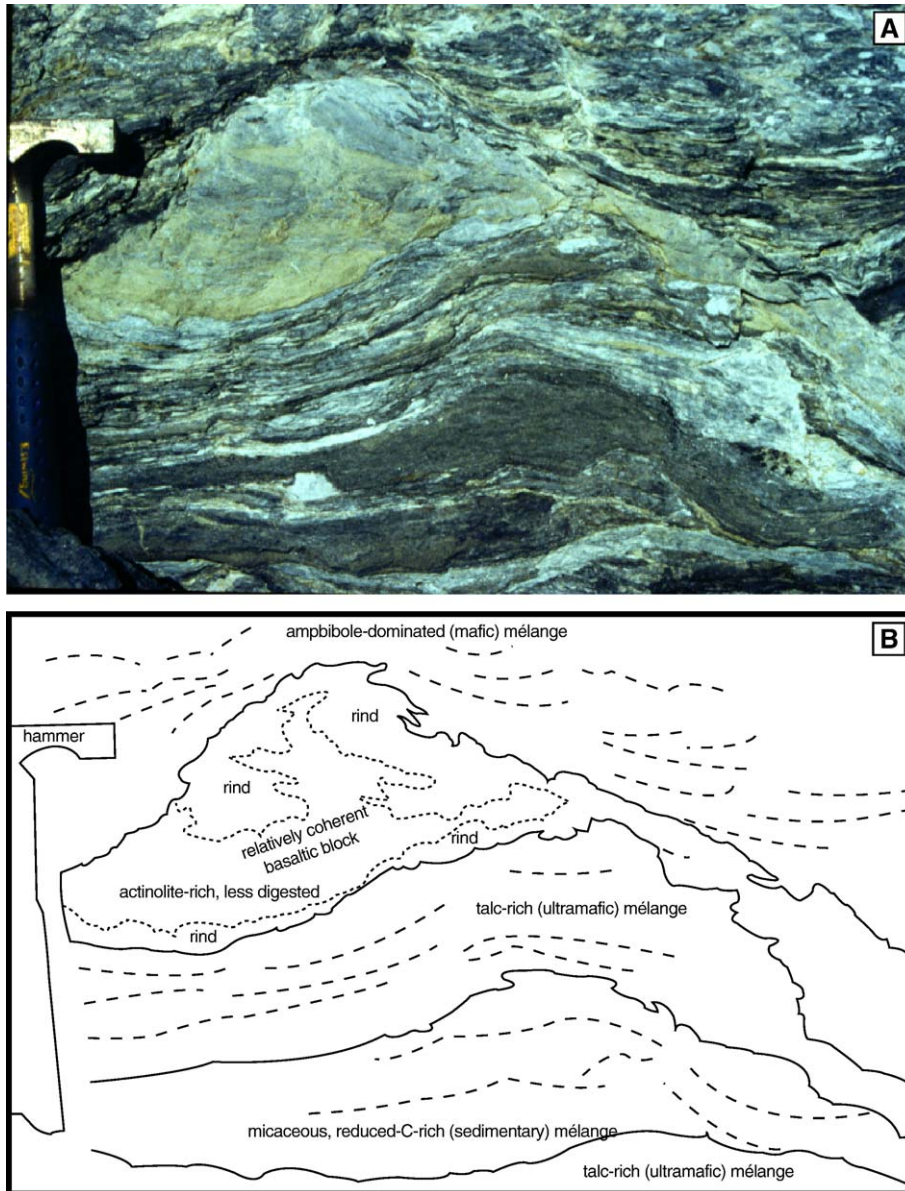


Fig. 1. Representative field photograph (A, above) and interpretative sketch (B, below) of meso-scale metamorphic and deformational features in lawsonite–albite facies *mélange* matrix of the Catalina Schist, CA. Solid lines denote contacts, dashed lines represent foliation. At left center is a large metabasaltic block bearing metasomatic rinds (dotted lines demarcate rind zones) within highly foliated *mélange* matrix. This exposure preserves amphibole-dominated (\sim mafic) *mélange* matrix, talc-dominated (\sim ultramafic) *mélange* matrix, and micaceous, reduced C-rich (\sim sedimentary) *mélange* matrix. Note that the coherent block records progressive disaggregation via boudinage, focused along rind/*mélange* contacts.

coherent basaltic and sedimentary blocks from the Catalina Schist [8,9,19] to samples of mélangé matrix in figures throughout this paper. Undigested peridotite blocks of the Catalina Schist have experienced a low-temperature serpentinization event subsequent to the subduction-related metamorphic history of interest and, as such, these compositions are unreliable for comparison to the mélangé matrix. We have chosen instead to represent the peridotite mixing end-member with the Horoman Peridotite Complex of Japan [32,33]. The Horoman complex is a depleted peridotite complex that has experienced varying degrees of cryptic metasomatic alteration that may be similar to subduction-related metasomatic enrichment of the mantle beneath arcs [32]. Application of the Horoman Complex as the peridotite end member in preliminary mixing models has indicated it is a reasonable choice and reliable alternative to the ultramafic blocks of the Catalina Schist [34]. In figures below, we present trends for simple mixing between the average Horoman peridotite with both the average Catalina basaltic and average Catalina sedimentary compositions to guide the reader to expected vectors for mechanical mixing in the mélangé.

Geochemical compositions of mélangé, however, are dependent on variables other than pure mechanical mixing and the mediating influence of metasomatism. These secondary processes can have competing effects on the geochemistry of mélangé zones and must be considered consistently when evaluating any individual sample. Foremost is the role of mélangé bulk composition, which strongly influences mineral stability [7,15].

Due to the prominent influence of ultramafic lithologies as part of the mélangé “protolith assemblage” comprising the Catalina Schist, many important trace element hosts may be destabilized as mélangé zones evolve to Mg-rich compositions [7]. This effect has also been clearly demonstrated in zones of mélangé outside of Catalina, where geochemical traverses along metasedimentary layers incorporated into an ultramafic mélangé reveal that the destabilization of metasedimentary micas results in preferential depletion of mica-compatible elements such as Rb, Cs, and Ba [15]. As such, even if a local zone of mélangé has incorporated a metasedimentary component rich in micas, the trace element character of this addition may not be evident in the analyzed sample if the new activity ratios buffered by the bulk composition resulted in mica breakdown and loss of this key elemental host [7,15]. Therefore, bulk composition represents one of the most significant controls on mélangé geochemistry.

Other processes likely have a subsidiary influence on geochemistry, but can dominate individual samples. Well-demonstrated in the Catalina Schist are elemental losses tied to the thermal structure of the subduction complex, where higher-grade equivalents contain proportionally lower elemental concentrations and diagnostic ratios, and these have been assigned to loss via prograde devolatilization [8,9]. For the Catalina mélangé matrix, devolatilization probably imparts a comparatively minor control as compared to bulk composition. Another process likely occurring during mélangé development is mass loss resulting from volume strain [7]. This “passive” process is believed to be largely responsible for relatively

Table 1
Mineralogical comparison between coherent blocks and mélangé zones

	Lawsonite–albite	Lawsonite–blueschist	Amphibolite
Coherent metasediment	Qtz + Ab + Chl + Wm + Lws ± Ca/Na-Amph	Qtz + Ab + Chl + Wm + Na-Amph + Lws	Qtz + Plag + Ky + Gt + Wm ± Btt
Coherent metamafic	Chl + Ab + Lws ± Ca/Na-Amph	Chl + Ab + Lws + Na-Amph	Hbd + Plag + Zo ± Gt
<i>Mélangé matrix</i> *			
Sediment-dominated	Chl ± Ab ± Qtz ± Gr ± Lws ± Wm ± Cc	Chl ± Ab ± Qtz ± Gr ± Na-Amph ± Ca/ Na-Amph ± Cc [Fch pods]	[not present]
Mafic-dominated	Ca/Na-Amph ± Lws ± Ab ± Chl ± Cc	Ca/Na-Amph ± Na-Amph ± Lws ± Chl ± Cc	Chl + Ca-Amph ± Tlc ± Btt
Ultramafic-dominated	Tlc ± Chl ± Ca-Amph ± Srp	Tlc ± Chl ± Fch ± Ca-Amph	Tlc + Act ± Chl ± Anth ± Ank ± En

Mineral Abbreviations for this table are as follows: Ab = albite, Act = actinolite, Ank = ankerite/dolomite, Anth = anthophyllite, Btt = biotite, Cc = calcite, Ca-amph = calcic amphibole ranging from actinolite to hornblende, Ca/Na-amph = calcic–sodic amphibole, Chl = chlorite, En = enstatite, Fch = fuchsite, Gl = glaucophane, Gr = carbonaceous matter (graphite in higher-grade units), Gt = garnet, Hbd = hornblende, Ky = kyanite, Lws = lawsonite, Mgs = magnesite, Plag = plagioclase, with An content higher than 10 mol.%, Qtz = quartz, Srp = serpentinite, Na-Amph = sodic amphibole, Tlc = talc, Wm = white mica (generally phengitic), and Zo = Zoisite/clinozoisite.

* Mélangé zones are highly variable in bulk composition and mineralogy. Mélangé matrix may contain abundant high-variance (nearly monomineralic) interlayers with these generalized mineralogies, depending on the relative proportions of metasedimentary, metamafic, and metaultramafic components. See the online dataset for petrographic descriptions of individual samples of mélangé matrix. Lawsonite–albite and lawsonite–blueschist samples of mélangé matrix contain variable amounts of apatite, rutile, and zircon. Amphibolite mélangé matrix is generally zircon-free, while apatite and rutile are common.

Al-rich ultramafic samples of AM mélange that are 90–95% modal chlorite and best interpreted as fluid-related restites that have been stripped of more fluid-mobile elements such as Si [7]. However, volume strain does not strictly imply loss of fluid-mobile elements. Two mélange samples (one is LA facies, the other LB facies) appear to have suffered extreme volume strain, leading to Cr contents of ~ 5 wt.%. These exceedingly high Cr contents have stabilized the Cr-rich white mica fuchsite, which strongly partitions Rb, Cs, and Ba, and concentrations of these elements in the Cr-rich samples are $\sim 10\times$ higher than other samples while almost all other trace elements have concentrations of < 1 ppm. These samples are consistent outliers in many of the diagrams discussed below, and provide a cautionary example that “protolith” compositions are strongly modified during mélange formation and mineral stability related to bulk composition is a dominant influence on geochemistry.

4. Elemental mixing systematics

4.1. Major element geochemistry

Major element compositions for mélange matrix of the Catalina Schist reflect protolith contributions inferred from field relations. Variations for selected major elements, plotted as a function of MgO (Fig. 2), indicate fundamental distinctions between the dominantly binary ultramafic–mafic AM-facies mélange mixture and ternary protolith mixtures expected for LB- and LA-facies mélange. We choose to present major element variations as a function of MgO in that the predominance of an ultramafic component within AM-facies mélange relative to lower-grade mélange provides for a first-order differentiation of the two types.

For the AM mélange, SiO_2 and Al_2O_3 compositions (Fig. 2A, B) indicate two distinct groups: one

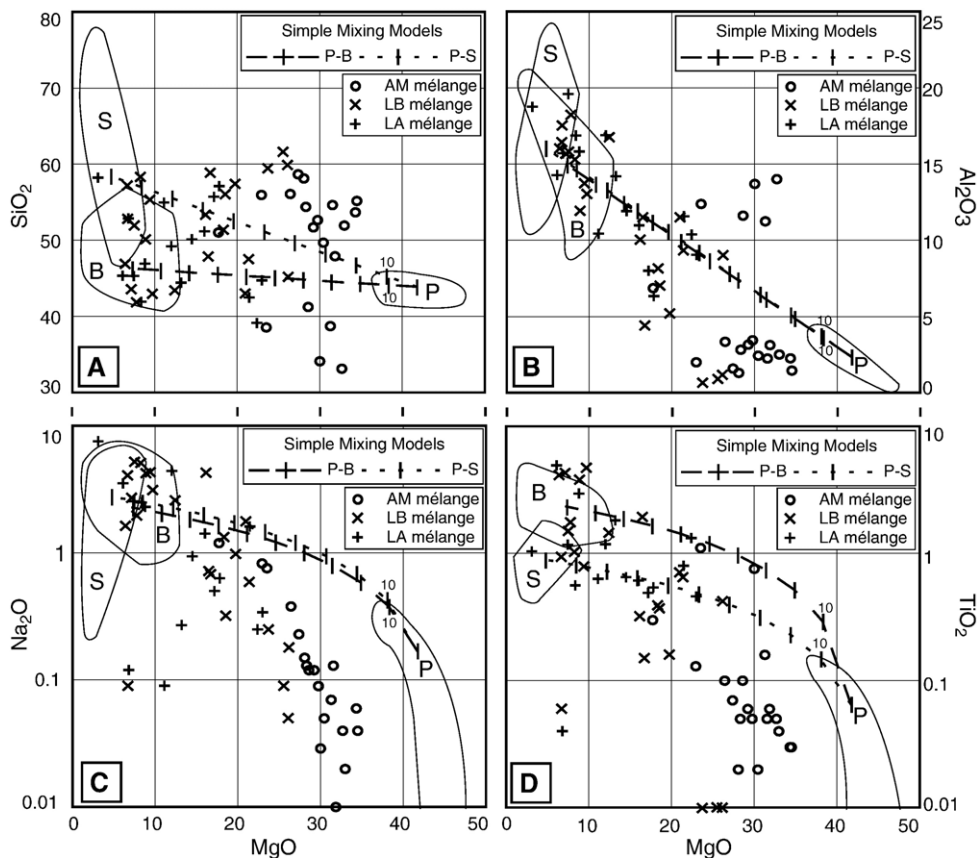


Fig. 2. Major-element compositions of Catalina Schist mélange matrix and comparison to the compositions of likely parental block end-members. Symbols as denoted in legends; AM, amphibolite-facies; LB, lawsonite–blueschist facies; LA, lawsonite–albite facies. Fields for parental end-members are as follows: B and S, basaltic and sedimentary blocks, respectively, of all metamorphic grades of the Catalina Schist; P, peridotites of the Horoman Complex, Japan. Simple mixing models are provided to demonstrate mechanical mixing vectors between average Horoman peridotite and both the average Catalina basaltic block (dashed line) and the average Catalina sedimentary block (dotted line), with crosses denoting 10% increments of the mixture. Only labels denoting the first 10% are shown for clarity. See text for explanation of mixing end members.

predominantly Si-rich, and Al-poor, the other with a much higher proportion of Al to Si. These variations are direct manifestations of the predominant mineralogy for these samples, where high-Si AM mélange is dominated by talc, whereas high-Al mélange is chlorite-rich. These mineralogic and geochemical effects are probably the result of competing enrichment and stripping processes occurring during mélange formation [7]. In contrast, LB and LA mélange appear to represent a continuous spectrum with no obvious co-variation between SiO₂ and MgO (Fig. 2A), but a distinct negative correlation between Al₂O₃ and MgO (Fig. 2B). This negative correlation is similar to what would be expected for evolution of an igneous suite; however, such a correlation within these rocks is indicative of different degrees of mechanical mixing between crustal components with an ultramafic component [7].

Variations of other incompatible major elements relative to MgO – represented by Na₂O and TiO₂ in Fig. 2C and D – demonstrate mechanical mixing vectors, but at concentrations generally below ideal mixing due to dilution primarily by SiO₂ enrichments and addition of structurally-bound H₂O. These mixing trends serve primarily to distinguish the compositional distinctions imposed upon the mélange matrix by the blocks available to matrix formation. We envision that these mixing trends are the direct result of metasomatic weakening of blocks through rind production [6,19] and mechanical incorporation of these comparatively weak metasomatic minerals into the developing mélange matrix [7], via distributed deformation mechanisms that are recognized or hypothesized to operate in phyllosilicates and amphiboles at plate-tectonic strain rates [29–31]. Conceivably, such protolith variations should be expressed within trace element and Sr–Nd isotope systematics.

4.2. Trace element geochemistry

Trace element diagrams further demonstrate that mélange formation produces hybridized rocks bridging compositional domains defined by likely protolith components. Concentration diagrams (Fig. 3) indicate that many elements are strongly controlled by phase stability. Compatible elements such as Cr and Ni (Fig. 3A) are excellent proxies for the dilution of the dominantly ultramafic AM mélange by crustal components, and the more complete range of the lower-grade LA/LB mélange, similar to major element variations (Fig. 2). Dilution of crustal components by an ultramafic influence is also monitored by incompatible elements such as Zr and Hf (Fig. 3B). Zr and Hf concentrations are low and highly variable in AM mélange, and this most likely reflects the

destabilization of zircon by the ultramafic bulk composition. Systematics for the mica-compatible elements Cs–Rb–B are very similar (Fig. 3C–D), reflecting the importance of the mica host. Mica is ubiquitous to samples of LA and LB mélange and stabilizes Cs–Rb–B concentrations very similar to the sedimentary and basaltic protoliths that dominate the budget for these elements during metamorphism. In contrast, the strongly ultramafic, mica-free AM mélange has low Cs–Rb–B concentrations and these elements do not strongly correlate, largely due to an absence of an ideal crystallographic host; however, concentrations are elevated compared to likely peridotite compositions, illustrating the hybridized compositions of the AM mélange. Other elements that are likely to experience strong control by single phases are Sr–U–Th–REE, which will partition into Ca-phases (lawsonite and apatite in LA/LB mélange; apatite only in AM mélange). For these elements (Fig. 3E–F), hybridization behavior is dominant, with most samples falling outside block compositions.

The ensuing role of elemental loss or depletion overprinting mixing behavior is difficult to uniquely assign to a single process (i.e., mineral host destabilization vs. prograde devolatilization), but the apparent loss of mass can be recognized in the mélange data. Ratios of mica-compatible LILE such as Cs and Ba to Th are insightful since Th has been demonstrated to be highly conservative even during extreme metasomatic depletions related to mélange formation [15]. Use of the Cs/Th or Ba/Th ratios as a function of respective LILE concentrations (Fig. 4A–B) indicate mixing vectors along the elemental axis, with resulting positive correlations that probably reflect preferential loss of LILE from micas. At present we are inclined to suggest that these correlations are a function of devolatilization rather than phase destabilization, as similar correlations exist for both the ultramafic AM mélange and the more crustal LA/LB mélanges, yet mica destabilization is less likely to occur within the relatively siliceous LA/LB mélanges.

Other variation diagrams utilizing ratios that involve Th are useful to discern the roles of protolith and fluid flow (Fig. 4C–D). The Th/Yb ratio strongly separates distinct protolith types along this axis, while ratios of Sr and Rb to Th illustrate two distinct types of geochemical behavior in mélange that are most likely tied to appropriate mineral hosts. Sr, Th, and Yb are probably all hosted by Ca-phases in all types of mélange, and the array present within Sr/Th–Th/Yb space reflects this similar behavior (Fig. 4C). However, ratios of these elements are consistently displaced to fields for basaltic and sedimentary coherent blocks in mélange regardless

of bulk composition. This is most pronounced within the strongly ultramafic AM mélange, where these ratios present a geochemical identity at odds with bulk composition. A similar diagram utilizing Rb/Th as a function of Th/Yb resolves what is essentially a mica fluid gain/loss vector along the Rb/Th axis versus the

compositional distinctions of Th/Yb (Fig. 4D). In this diagram, lower-grade LA/LB mélange appears dominantly sedimentary with variations in Rb/Th most likely resulting from the modal abundance of mica. A broad array extending from the peridotite block field formed by the AM mélange in this space suggests an important

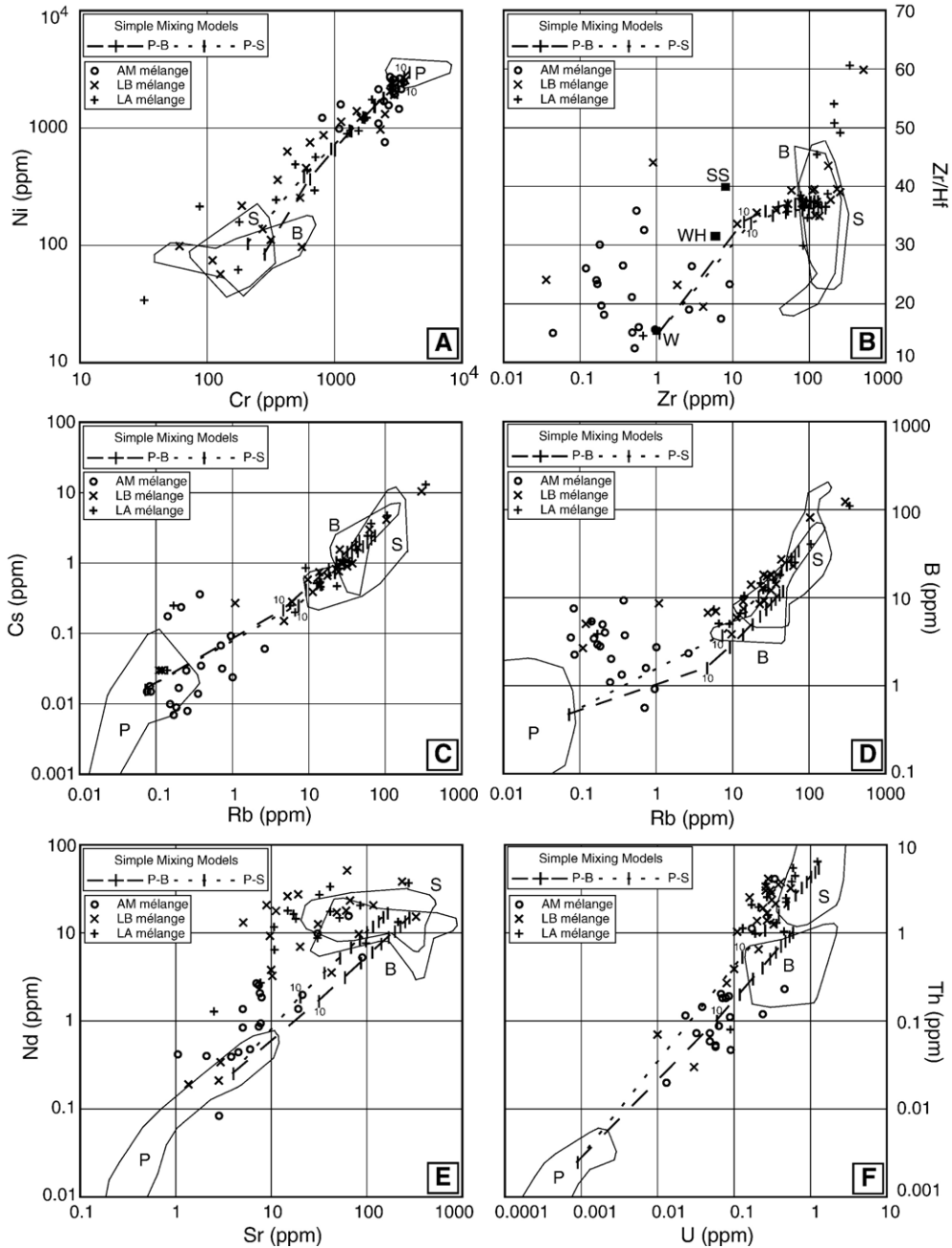


Fig. 3. Trace-element variation diagrams of the Catalina Schist mélange matrix; symbols, labeled fields, and simple mixing models for parental blocks follow the convention of Fig. 2. Black squares in 3B are proposed Zr–Hf compositions for the depleted mantle; SS = Salters and Stracke [35]; W = Weyer et al. [36]; WH = Workman and Hart [37].

mixing component in the AM *mélange* was derived from a source with a sub-sedimentary Rb/Th ratio. This component is probably that of sedimentary-derived fluids; similar fluids affecting the AM *mélange* have been inferred from previous investigations of the Catalina Schist [4–7], although our current data suggest this sedimentary source had previously experienced Rb loss, probably related to previous devolatilization.

A recent paper by Plank [38] has demonstrated the utility of Th–La–Sm systematics as an indicator of contamination by subducted sediment in the source of arc magmatic systems, and we have explored these same discrimination diagrams with our data (Fig. 5). These systematics should work equally as well in the *mélange*, as this environment displays clear geologic evidence for mixing of sediment and peridotite. However, Th–La–Sm systematics do not appear to be sensitive to *mélange* mixing processes. This may primarily reflect high apparent degrees of sediment incorporation in the *mélange* (i.e., >10%), as even these small extents of

sediment incorporation overwhelm peridotite compositions. The most important result of the application of these systematics to the *mélange* is that while small extents of sediment incorporation significantly alter these trace element ratios, major element compositions (as proxied by MgO; Fig. 5B) are not significantly displaced, implying phase equilibria similar to an ultramafic system. This implies that sedimentary-like compositions could erroneously be inferred as contaminants to an arc magmatic source, as the trace element ratios do not uniquely identify sediment contributions. Therefore, the mixing trajectories of Plank [38] can just as easily be explained by contamination of arc magma sources regions from *mélange* zones of very different bulk composition than an ideal sediment, where not all trace element ratios of the contaminant could be predicted from a model sediment composition. We discuss the full ramifications of these data below.

To summarize the *mélange* trace element data, we present a series of NMORB-normalized [39] incompatible

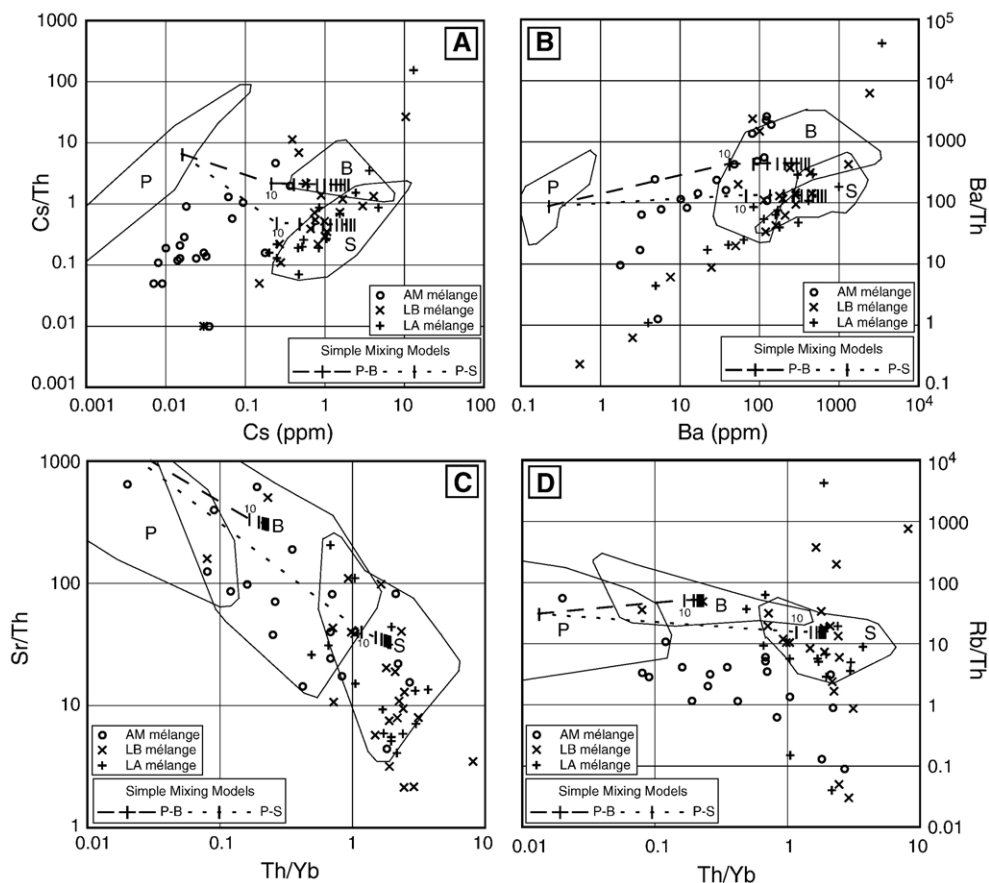


Fig. 4. Trace-element variation diagrams of the Catalina Schist *mélange* matrix; symbols, labeled fields, and simple mixing models for parental blocks follow the convention of Fig. 2.

element diagrams for a range of mélangé compositions and selected geochemical reference compositions (Fig. 6). Mélangé compositions presented in Fig. 6 encompass the full range in elemental concentrations for each unit and display characteristic patterns. LREE enrichment is a common feature of mélangé, as are distinct anomalies for many fluid-mobile elements such as Cs, Rb, Ba, B, Pb, Sr, and Li. Cs–Rb–Ba data for amphibolite mélangé are incoherent as compared to lower grades of mélangé, which we interpret to be a reflection of the mica-free amphibolite assemblages. Phase-controlled anomalies of HFSE are most readily apparent within amphibolite-facies mélangé, where the absence of zircon and/or rutile from the bulk composition imparts significant negative HFSE anomalies, implying HFSE loss. These diagrams illustrate the overall geochemical character of the Catalina Schist mélangé matrix and demonstrate the important control of geochemistry by phase stability.

5. Sr–Nd isotope geochemistry

In this contribution we report Sr–Nd isotope ratios as age-corrected initial ratios based upon existing white mica Ar–Ar closure ages [18]. Unique ages for each sample are not available, so we have chosen to present maximum and minimum age corrections based on the range in Ar–Ar ages for each unit [18]. The range in age corrections spans 15 Ma in all cases.

When viewed on a ϵNd vs. $^{87}\text{Sr}/^{86}\text{Sr}$ isotope variation diagram, no firm array in the mélangé data is

evident (Fig. 7). However, the isotope data do display a consistent displacement away from likely oceanic isotope signatures (i.e., \sim MORB) to lower ϵNd and higher $^{87}\text{Sr}/^{86}\text{Sr}$ characteristic of the continental crust. The most striking feature of the data is that no correlation exists between inferred protolith contributions as inferred from field relations, mineralogy, and major element data (Table 1, Fig. 2) and all samples are essentially indistinguishable. Isotopic compositions are similar to previously reported Sr–Nd initial ratios for other subduction-related metabasaltic eclogites and blueschists, [40–42] suggesting modification of pre-subduction isotopic compositions by subduction-zone metamorphism is a common feature.

Isotope-element mixing diagrams provide substantial insight into the processes and origins of Sr–Nd isotopic signatures of the Catalina Schist mélangé matrix. Comparison of age-corrected $^{87}\text{Sr}/^{86}\text{Sr}$ vs. $1/\text{Sr}$ (Fig. 8A) indicates three dominant end-members were involved during mélangé formation. We interpret that an approximately binary mixing array between a low-Sr concentration, radiogenic $^{87}\text{Sr}/^{86}\text{Sr}$ (~ 0.711) end-member with a median Sr, nonradiogenic (~ 0.702) source probably represents a mechanical mixing vector within the mélangé. This array is intersected by a strong, high-Sr concentration signal at an $^{87}\text{Sr}/^{86}\text{Sr}$ ratio of 0.705–0.706 that most likely represents the dominant metasomatic fluid composition. These inferences are corroborated by the insensitivity of the “fluid” $^{87}\text{Sr}/^{86}\text{Sr}$ to the Sr/Th ratio (consistent with fluid additions of Sr and relative immobility of Th; Fig. 8B), while the other two end-

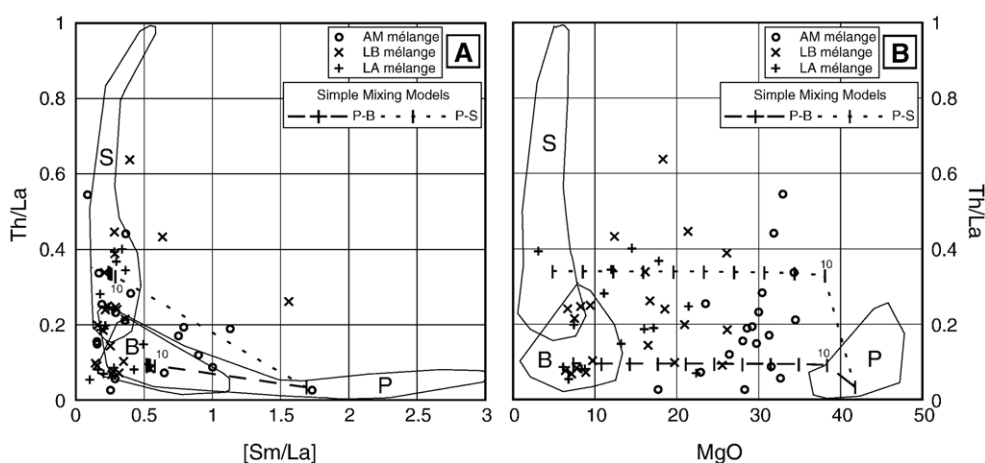


Fig. 5. Th/La vs. [Sm/La] (left, A, see [38]) and Th/La vs. MgO (right, B) for mélangé matrix. Symbols, labeled fields, and simple mixing models for parental blocks follow the convention of Fig. 2. Compared to [38], Th–La–Sm systematics do not uniquely identify sedimentary contributions in mixing processes. Furthermore, Th/La is independent of bulk composition for mixing proportions of $>10\%$ of basalt and sediment (as proxied by MgO) illustrating that this ratio may be an unreliable indicator of the role of sediments in subduction-zone processes. [Sm/La] normalized to the NMORB values of [39].

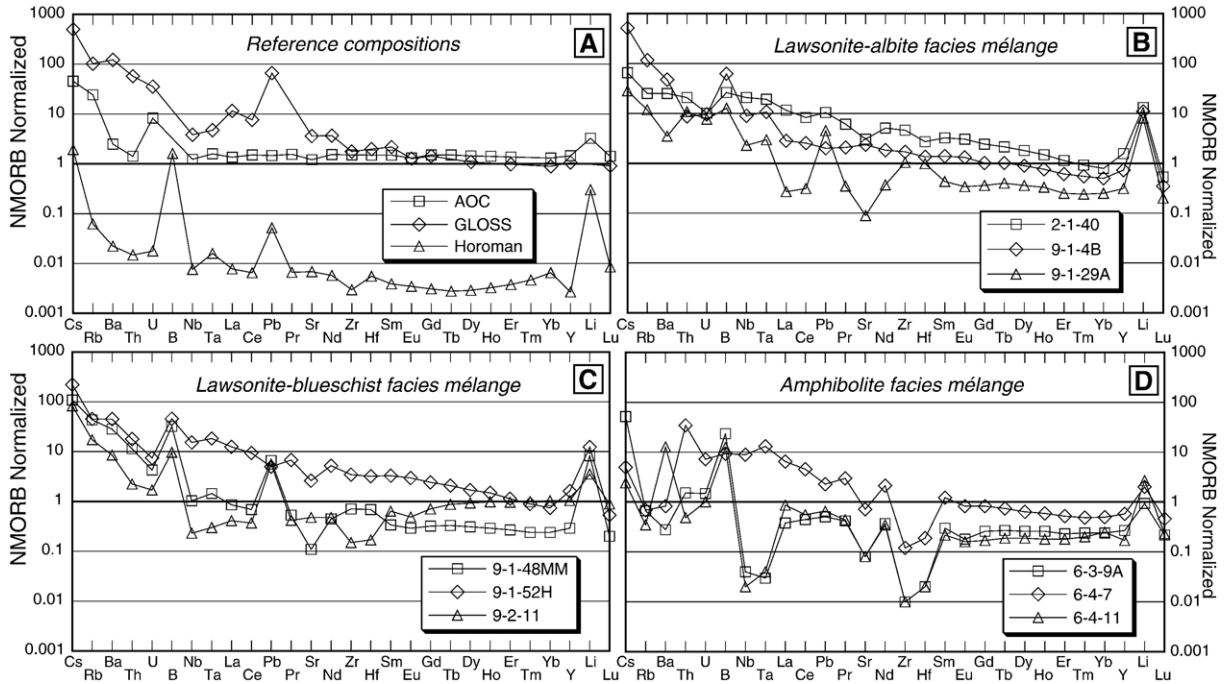


Fig. 6. NMORB-normalized [39] incompatible element diagrams for geochemical reference compositions (A) and mélange matrix of the Catalina Schist (B–D). Reference compositions in A are the altered oceanic crust (AOC) composite of [3], estimated composition of global subducting sediment (GLOSS) of [2], and a depleted mantle composite composition (Horoman) based on the Horoman Peridotite complex of Japan [32,33] and depleted mantle data of [36]. Compositions for mélange matrix were chosen to express typical incompatible element patterns and the full range in concentrations observed in each unit.

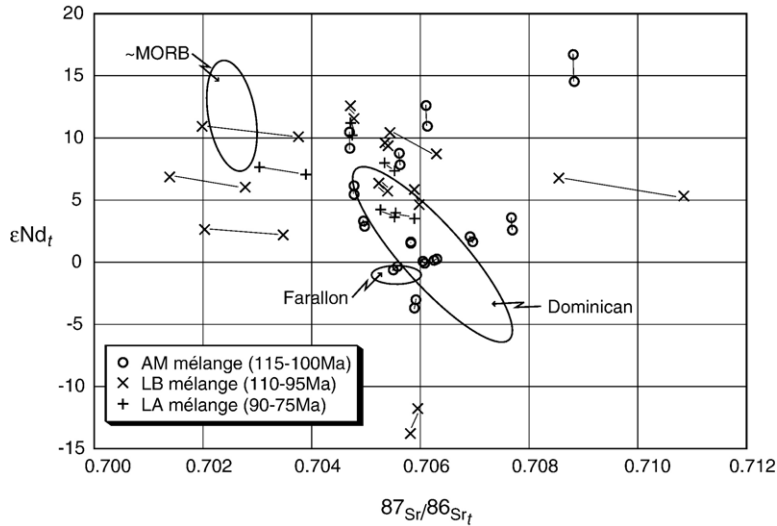


Fig. 7. Sr–Nd isotope data for mélange matrix of the Catalina Schist presented as initial isotope ratios. Isotope compositions are age corrected for a range in ages due to uncertainty in the precise age of the mélange matrix; age ranges based on Ar–Ar closure ages of [18]. Lines connect age corrections of individual samples; symbols and ages for correction given in the legend. Errors based upon age corrections greatly exceed all analytical errors. Oval labeled “MORB” represents an approximate Sr–Nd composition for mid-ocean ridge basalts. Oval labeled “Farallon” indicates the range in Sr–Nd composition for omphacite mineral separates from lawsonite eclogite xenoliths from the Colorado Plateau demonstrated to have originated as fragments of the subducted Farallon plate and of approximate MORB parentage [41,42]. Oval labeled “Dominican” is for the Sr–Nd compositions of metabasaltic blueschists and eclogites of the Dominican Republic as reported by [40].

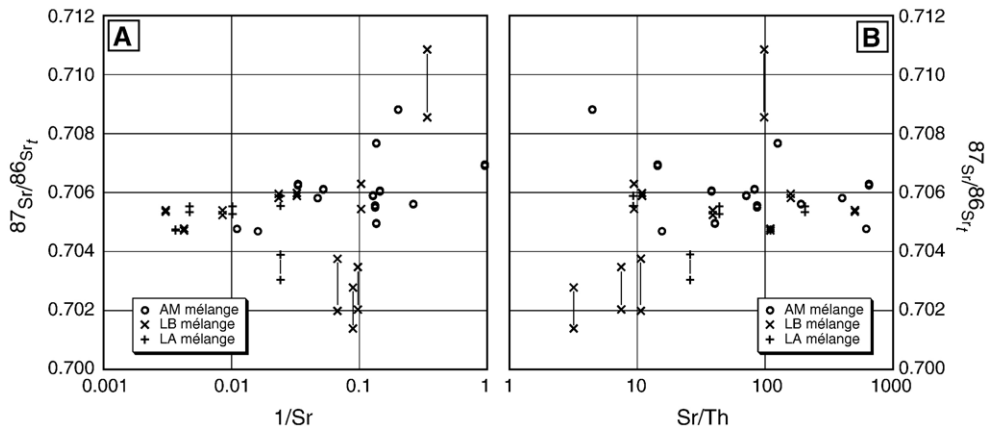


Fig. 8. Sr isotope-element mixing diagrams. Tie lines are shown connecting the two age corrections used for each sample; tie lines are not shown for samples where the two symbols overlap. See text for details regarding age correction of isotope ratios. Sr isotope ratios as a function of inverse Sr concentration (left, A) suggest a likely mechanical mixing array overprinted by a high-Sr-concentration fluid signal of ~ 0.705 – 0.706 . This inferred fluid signal is largely independent of Sr/Th (right, B), also suggestive of a fluid source.

members may preserve distinct Sr/Th ratios associated with their source.

Nd mixing arrays suggest two-component mixing (Fig. 9), although correlations are imperfect and the end-member compositions are unexpected. End-members involved in mixing are a positive ϵNd ($\sim +15$), high-Nd concentration, LREE enriched source, while the second has negative ϵNd (~ -10), low-Nd concentration, and is LREE depleted. The simplest interpretation of the two “mechanical” end-members in both Sr and Nd mixing diagrams is that the first end member – having low $^{87}\text{Sr}/^{86}\text{Sr}$, positive ϵNd , and LREE enrichment – is some type of

altered oceanic crust, while the high $^{87}\text{Sr}/^{86}\text{Sr}$, negative ϵNd , LREE depleted component is a crustal, likely continental, component that experienced a previous devolatilization event promoting Sr and LREE loss. These apparent mixing components are identifications that require refinement, but most simply explain the existing data.

6. Mélange and the slab–mantle interface

Prior to any discussion of the geochemistry of the mélange zones of the Catalina Schist, it is worthwhile to briefly discuss why mélange will form in all subduction

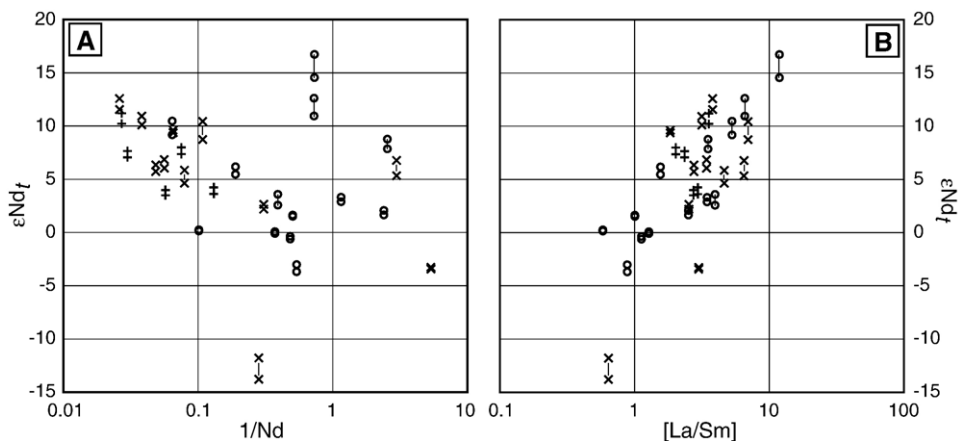


Fig. 9. Nd isotope-element mixing diagrams. Tie lines are shown connecting the two age corrections used for each sample; tie lines are not shown for samples where the two symbols overlap. See text for details regarding age correction of isotope ratios. Nd data suggest a binary mixing array between a positive ϵNd , high Nd concentration, LREE-enriched source with a negative ϵNd , low Nd concentration, LREE-depleted composition. The mixing array is probably controlled by mechanical mixing as little evidence for modification of this array by fluid flow is evident, in contrast to our interpretation of Sr isotope systematics.

zones, and the physical role these *mélange* zones will have in the overall subduction system. *Mélange* must intrinsically form along the slab–mantle interface to form the chemical bridge between the depleted peridotites of the mantle wedge and the evolved components of the subducting slab. Across this interface, severe contrasts exist in the chemical potentials of essentially every chemical species, but most notably for incompatible major and trace elements and their isotopic ratios, as well as volatile components. Due to these thermodynamic constraints, a gradient formed through some mechanism must accommodate the physical juxtaposition of these distinct chemical reservoirs. This gradient may be expressed as a simple metasomatic buffering zone formed in the mantle wedge [43–47], but a more complicated scenario further involving mechanical deformation and the formation of *mélange* [5–7] is much more likely given the likelihood of distributed deformation dominating along the slab–mantle shear zone owing to the presence of rheologically weak minerals formed during metamorphism [29–31].

In all these scenarios, fluids are required as agents of mass transfer to resolve the chemical gradient across the slab–mantle interface. However, conflicting results regarding fluid release within metamorphosed subduction complexes have questioned the extent of fluid mobility within the subducting section. One group of studies finds that fluid flow and elemental mobility are linked and measurable geochemical depletions develop during subduction [8–11,15,48–50] or that pervasive fluid flow and large fluid fluxes are required to explain strongly homogenized stable isotope compositions or high-variance metasomatic structures, including *mélange* [4–7,47]. Conversely, numerous studies of largely eclogite-facies rocks find no evidence for large-scale fluid flow in that either measurable geochemical depletions are completely absent [12,13,51], fluids are retained by the rock or fluid connectivity is extremely low [52], or that preservation of stable isotopic homogeneities imparted by the protolith are retained even to ultrahigh-pressure conditions [53]. Perhaps these differences are not strongly at odds, since fluid flow is generally observed in areas of strong metasomatism associated with abundant fluid-flow structures, while sites of restricted or no fluid flow are commonly large blocks or modest tracts of material with few observable permeability structures. Accordingly, some authors have suggested that null results for fluid mobility from tectonic blocks in subduction complexes are the result of highly localized fluid pathways that are preferentially destroyed during exhumation [54,55], and this interpretation infers the presence of fossil *mélange* zones in the complex. Our present interpretation of the

existing research is that fluid mobility and geochemical modification is restricted to high permeability pathways such as *mélange* zones and fractures, and that comparatively minor evidence for mobility will be observed in tectonic blocks. As such, digestion of tectonic blocks leading to *mélange* formation can be viewed as a crucial component for fluid and elemental mobility within subduction complexes [5–7,15].

Therefore, it appears much more plausible that fluid mobility is dominant in hybridized *mélange* zones, implying that *mélange* zones are a more likely source for fluids promoting arc magmatism. This conclusion raises two significant dilemmas linked to the complexities inherent to *mélange* formation: chemical heterogeneities produced by the process and the highly unpredictable phase equilibria associated with such a wide range in composition. At present, it is difficult to assess the departure of phase relations of key trace-element hosts (such as phengitic white mica) from existing constraints as little motive has previously existed to investigate phase relations in novel bulk compositions such as those we report here. We discuss the connections between the geochemistry of *mélange* and other components in the subduction system below.

7. The role of *mélange* in the subduction system

The dominant approach many utilize to resolve geochemical recycling during subduction is a comparison of subduction inputs vs. subduction outputs, usually to resolve what subducted lithologies are important contributors to the arc magmatic system or to constrain what proportion of subducted material is returned to the deep mantle (e.g. [1–3,38,56–61]). Many of these studies are limited by our inadequate understanding of the physical processes accommodating mass transfer within the trench-to-subarc metamorphic system, so that a common assumption is that pre-subduction ocean-floor lithologies retain their geochemical character during subduction, and that these lithologic components can then be resolved using characteristic elemental or isotopic tracers evident in arc volcanics as indicators of their involvement in arc magmatogenesis. However, as we demonstrate in this contribution, subduction-zone metamorphism consistently redistributes mass to form hybridized rock types with no correlative protolith within the pre subduction lithologic section, the phase equilibria of this system are not established, and it is within these hybridized rock types that fluid flow most likely occurs. This raises numerous points for our ensuing discussion: How will the heterogeneous composition of *mélange* zones

impact the chemistry of fluid/liquid phases interacting with or derived from *mélange*? Are characteristic ratios of particular pre-subduction lithologies retained during *mélange* formation? Is there utility in expressing slab-derived components as a mixture of sediment or altered oceanic crust? We consider these questions below.

As is obvious from our data, significant heterogeneities are a fundamental product of *mélange*-forming processes. The composition of any given zone of *mélange* primarily will be a function of the composition of neighboring blocks “feeding” the *mélange* zone, further mediated by metasomatic vectors. The activity ratios buffered by the *mélange* zone will be the most important control on phase stability [7] and, therefore, trace element compatibility in the *mélange* and mobility in fluids. As directly observed by Breeding et al. [15], micas are destabilized when they are digested by an ultramafic bulk composition, resulting in near-complete loss of mica-compatible elements such as K, Rb, Cs, and Ba from the *mélange*. This process is not limited to micas, and is likely to occur whenever activity ratios are suitably modified so that mineral hosts are no longer stable. We can consider this process and extrapolate our reasoning to consider the behavior of zircon within *mélange* zones and apply *mélange* processes as a potential explanation for Hf isotope anomalies in some volcanic arcs using a thought experiment. Consider the current problem of measured Hf isotope anomalies within some arc volcanic centers that implicate derivation of Hf from a subducted component [62,63]. In some cases these anomalies are restricted to volcanoes interpreted to be influenced by slab melts [63], although Hf anomalies are also associated with volcanoes solely influenced by a hydrous fluid metasomatic agent [62]. Any mobility of Hf in hydrous fluids will be a function of both the stability of zircon as a host for Hf within the metamorphic system and the presence of solvating ligands such as halogens to promote Hf solubility [64]. It appears that the stability of zircon in ultramafic assemblages such as these *mélange* units has a lower limit at a SiO_2 activity (a_{SiO_2}) buffered by a talc-tremolite metasomatic reaction [47]. Therefore, one interpretation of the arc Hf isotope data is simply that Hf mobility is associated with subduction zones where a_{SiO_2} in *mélange* is buffered by talc + chlorite assemblages and zircon is absent, whereas zircon is stable and Hf is retained in more siliceous *mélange*. Therefore, mechanical incorporation of a slab-derived zircon into an ultramafic zone of *mélange* may destabilize the zircon due to activity ratios, mobilizing zircon-derived, crustal Hf to the arc. Our *mélange* Zr–Hf data (Figs. 3B, 6) appear to support this interpretation as more siliceous samples preserve much higher concentrations of Zr–Hf at a relatively constant Zr/Hf ratio, while Zr–Hf concentrations are low

and Zr/Hf ratios are variable in more ultramafic samples that lack zircon; this variability most likely reflects some Zr–Hf mobility in the absence of zircon.

We focus on the role of mineral hosts in *mélange* as they ultimately control all trace element systematics of the system. This contrasts a pervasive convention in a significant portion of the literature that identifies contaminants to the arc magmatic system as “sediments” or “altered oceanic crust.” Although this convention is convenient as comparisons to subduction-zone inputs [1–3] can be made and mass-balance constraints employed to determine the overall fate of subducted mass, this approach strongly de-emphasizes the fundamental physical processes – that is, mineral reactions – mobilizing material to the arc source. The importance of a physical basis for mass transfer in the subduction system is only highlighted by the *mélange* data, which demonstrate that mass is consistently redistributed during metamorphism to form hybridized lithologies, and it is within these *mélange* zones where metasomatic agents such as hydrous fluids, silicate liquids, or miscible supercritical phases are probably concentrated. As our new data demonstrate, these reservoirs can be dismembered and reorganized as *mélange*, which can then bear isotopic or elemental indicators of numerous “reservoirs” in a bulk composition not reminiscent of any protolith. Consider a sample of AM *mélange*, 6-3-33: This sample is very ultramafic ($\text{SiO}_2=41.27\%$, $\text{MgO}=28.57\%$) chlorite + anthophyllite + talc schist that is mica-free with low major-element alkalis ($\text{Na}_2\text{O}=0.12\%$, $\text{K}_2\text{O}=0.02\%$), bears Th/La (0.19) and Th/Yb (0.26) ratios consistent with this composition, yet presents Sr–Nd isotope systematics reminiscent of a more evolved rock ($^{87}\text{Sr}/^{86}\text{Sr}=0.70590$, $\epsilon_{\text{Nd}}=-3.30$). A second example is another AM *mélange* sample (6-3-60) that is also Mg-rich, but with a more siliceous mineralogy of talc + chlorite + enstatite ($\text{SiO}_2=51.96\%$, $\text{MgO}=32.94\%$), has high Th/La (0.545) reminiscent of sediments, a very mantle-like Nd isotopic ratio (+15.66), yet radiogenic $^{87}\text{Sr}/^{86}\text{Sr}$ (0.70882). These examples preserve diagnostic ratios of multiple pre-subduction input sources, none of which are characteristic of the sample. Due to these compositions, it is difficult to discern whether effective contaminants calculated from arc volcanic data represent proportions of real contributions from the pre-subduction section, or if they simply reflect the signature of a hybridized rock. Therefore, the mediating action of subduction-zone metamorphic processes such as *mélange* formation can significantly complicate assumptions based upon the seafloor geochemical record due to the aggradation of mass into a hybridized composition. Our continuing research based on these samples aims to quantitatively

resolve pre-subduction compositions inherited by mélange in order to derive a process-driven model applicable to subduction zones worldwide, but to date these attempts have produced unsatisfactory results. We hope that the presentation of these complicated data to the community results in alternative theories for mélange formation, which may allow for new directions in subduction zone research.

8. Conclusions

We have investigated the geochemical ramifications of subduction-zone mélange formation as recorded by the mélange matrix of the Catalina Schist, CA. The bulk compositions of these samples are consistent with their demonstrated petrogenesis and similar mélange zones are probably ubiquitous to subduction zones worldwide. Our major conclusions are:

1. Mélange formation results in hybridized rock types that are not representative of the incoming subduction section, yet mélange commonly retains geochemical signals characteristic of one or more “input” components.
2. The dominant control on the geochemistry of any mélange zone will be the mineral stabilities buffered by major-element bulk composition. Mélange zones may naturally evolve in a manner to stabilize or de-stabilize minerals that will be important trace-element hosts.
3. When compared to the record of coherent lithologies in subduction complexes, fluid flow and metasomatic alteration are much more strongly expressed within mélange, suggesting mélange probably acts as the dominant high-permeability pathway for mobile phases during subduction.
4. Elemental “mobility” in subduction zones is probably a function of appropriate mineral hosts for element residency within mélange. As activity ratios vary in the evolution of mélange, mobility will vary with bulk composition and phase equilibria.
5. Comparisons of subduction “inputs” vs. “outputs” are of limited utility if the reaction pathways of mass transfer during metamorphism are not considered. As material is processed thorough mélange formation, discrete entities such as “subducted sediment” or “altered oceanic crust” are disrupted, modified, and may cease to exist as perceived from the pre-subduction record. While these input compositions will be important initial conditions of future process models that are able to predict mélange compositions at depth, the current state of their physical link to arc volcanism needs to be better demonstrated.

Acknowledgments

We thank the many people who have participated in lively discussion of our data at meetings over the past three years. RLK would like to thank C. Sakaguchi for patience and guidance during TIMS analyses, all the members of the PML for constant support and criticism, and M. Walter for rational discussions of geochemistry and petrogenesis. Formal reviews by Jay Ague, Terry Plank, and the editorial handling of Ken Farley improved the manuscript, although they do not agree with all of our interpretations. This study was funded by grants from the U.S. National Science Foundation (EAR-0079331, to Bebout) and from the 21st Century of Excellence Program, Japanese Ministry of Education, Science, Sports, and Culture (to Nakamura).

Appendix A. Supplementary data

Supplementary data associated with this article can be found, in the online version, at [doi:10.1016/j.epsl.2006.03.053](https://doi.org/10.1016/j.epsl.2006.03.053).

References

- [1] D.K. Rea, L.J. Ruff, Composition and mass flux of sediment entering the world’s subduction zones: implications for global sediment budgets, great earthquakes, and volcanism, *Earth Planet. Sci. Lett.* 140 (1996) 1–12.
- [2] T. Plank, C.H. Langmuir, The chemical composition of subducting sediment: implications for the crust and mantle, *Chem. Geol.* 145 (1998) 325–394.
- [3] K.A. Kelley, T. Plank, J. Ludden, H. Staudigel, Composition of altered oceanic crust at ODP sites 801 and 1149, *Geochem. Geophys. Geosyst.* 4 (2003) [doi:10.1029/2002GC000435](https://doi.org/10.1029/2002GC000435).
- [4] G.E. Bebout, Field-based evidence for devolatilization in subduction zones: implications for arc magmatism, *Science* 251 (1991) 413–416.
- [5] G.E. Bebout, M.D. Barton, Fluid flow and metasomatism in a subduction zone hydrothermal system, Catalina Schist terrane, California, *Geology* 17 (1989) 976–980.
- [6] G.E. Bebout, M.D. Barton, Metasomatism during subduction: products and possible paths in the Catalina Schist, California, *Chem. Geol.* 108 (1993) 61–92.
- [7] G.E. Bebout, M.D. Barton, Tectonic and metasomatic mixing in a subduction-zone mélange: insights into the geochemical evolution of the slab–mantle interface, *Chem. Geol.* 187 (2002) 79–106.
- [8] G.E. Bebout, J.G. Ryan, W.P. Leeman, B–Be systematics in subduction-related metamorphic rocks: characterization of the subducted component, *Geochim. Cosmochim. Acta* 57 (1993) 2227–2237.
- [9] G.E. Bebout, J.G. Ryan, W.P. Leeman, A.E. Bebout, Fractionation of trace elements by subduction-zone metamorphism—effect of convergent-margin thermal evolution, *Earth Planet. Sci. Lett.* 171 (1999) 63–81.
- [10] H. Becker, J.P. Jochum, R.W. Carlson, Constraints from high-pressure veins in eclogites on the composition of hydrous fluids in subduction zones, *Chem. Geol.* 160 (1999) 291–308.

- [11] H. Becker, J.P. Jochum, R.W. Carlson, Trace element fractionation during dehydration of eclogites from high-pressure terranes and the implications for element fluxes in subduction zones, *Chem. Geol.* 163 (2000) 65–99.
- [12] C. Spandler, J. Hermann, R. Arculus, J. Mavrogenes, Redistribution of trace elements during prograde metamorphism from lawsonite blueschist to eclogite facies; implications for deep subduction-zone processes, *Contrib. Mineral. Petrol.* 146 (2003) 205–222.
- [13] C. Spandler, J. Hermann, R. Arculus, J. Mavrogenes, Geochemical heterogeneity and element mobility in deeply subducted oceanic crust; insights from high-pressure mafic rocks from New Caledonia, *Chem. Geol.* 206 (2004) 21–42.
- [14] D.M. Fisher, Fabrics and veins the forearc: a record of cyclic fluid flow at depths of <15 km, in: G.E. Bebout, D.W. Scholl, S.H. Kirby, J.P. Platt (Eds.), *Subduction top to bottom*, AGU Geophysical Monograph, vol. 96, 1996, pp. 75–89.
- [15] C.M. Breeding, J.J. Ague, M. Bröcker, Fluid–metasedimentary rock interactions in subduction-zone mélange: implications for the chemical composition of arc magmas, *Geology* 32 (2004) 1041–1044.
- [16] G.A. Abers, Hydrated subducted crust at 100–250 km depth, *Earth Planet. Sci. Lett.* 176 (2000) 323–330.
- [17] B.O. Mysen, P. Ulmer, J. Konzett, M.W. Schmidt, The upper mantle near convergent plate boundaries, in: R.J. Hemley (Ed.), *Ultra-high-pressure mineralogy*, Mineralogical Society of America, 1998, pp. 97–138.
- [18] M. Grove, G.E. Bebout, Cretaceous tectonic evolution of coastal southern California: insights from the Catalina Schist, *Tectonics* 14 (1995) 1290–1308.
- [19] S.S. Sorensen, J.N. Grossman, Enrichment of trace elements in garnet amphibolites from a paleo-subduction zone: Catalina Schist, southern California, *Geochim. Acta* 53 (1989) 3155–3177.
- [20] H. Takei, Development of precise analytical techniques for major and trace element concentrations in rock samples and their applications to the Hishikari gold mine, southern Kyushu, Japan [Ph.D. thesis]: Misasa, Japan, University of Okayama at Misasa.
- [21] T. Yokoyama, A. Makishima, E. Nakamura, Evaluation of the coprecipitation of incompatible trace elements with fluoride during silicate rock dissolution by acid digestion, *Chem. Geol.* 157 (1999) 175–187.
- [22] A. Makishima, E. Nakamura, Suppression of matrix effects in ICP-MS by high power operation of ICP: application to precise determination of Rb, Sr, Y, Cs, Ba, REE, Pb, Th, and U at ng g^{-1} levels in milligram silicate samples, *Geostand. Newsl.* 21 (1997) 307–319.
- [23] T. Moriguti, A. Makishima, E. Nakamura, Determination for lithium contents in silicates by isotope dilution ICP-MS and its evaluation by isotope dilution TIMS, *Geostand. Newsl.* 28 (2004) 371–382.
- [24] A. Makishima, E. Nakamura, T. Nakano, Determination of boron in silicate samples by direct aspiration of sample HF solutions into ICPMS, *Anal. Chem.* 69 (1997) 3754–3759.
- [25] A. Makishima, E. Nakamura, T. Nakano, Determination of zirconium, niobium, hafnium, and tantalum at ng g^{-1} levels in geological materials by direct nebulisation of sample HF solution into FI-ICP-MS, *Geostand. Newsl.* 23 (1999) 7–20.
- [26] R. Tanaka, A. Makishima, H. Kitagawa, E. Nakamura, Suppression of Zr, Nb, Hf and Ta coprecipitation in fluoride compounds for determination in Ca-rich materials, *J. Anal. At. Spectrom.* 18 (2003) 1458–1463.
- [27] M. Yoshikawa, E. Nakamura, Precise isotope determination of trace amounts of Sr in magnesium-rich samples, *J. Mineral. Petrol. Econ. Geol.* 88 (1993) 548–561.
- [28] A. Makishima, E. Nakamura, Precise measurement of cerium isotope composition in rock samples, *Chem. Geol.* 94 (1991) 1–11.
- [29] L.A. Reinen, Seismic and aseismic slip indicators in serpentinite gouge, *Geology* 28 (2000) 135–138.
- [30] L.A. Reinen, T.E. Tullis, J.D. Weeks, The frictional behavior of antigorite and lizardite serpentinite: experiments, constitutive models, and implications for natural faults, *Pure Appl. Geophys.* 143 (1994) 317–358.
- [31] S.M. Peacock, R.D. Hyndman, Hydrous minerals in the mantle wedge and the maximum depth of subduction thrust earthquakes, *Geophys. Res. Lett.* 26 (1999) 2517–2520.
- [32] M. Yoshikawa, E. Nakamura, Geochemical evolution of the Horoman peridotite complex: implications for melt extraction, metasomatism and compositional layering in the mantle, *J. Geophys. Res.* 105 (2000) 2879–2901.
- [33] M. Tanimoto, Petrology and geochemistry of the Horoman peridotite complex, Hokkaido, northern Japan [M.S. thesis]: Misasa, Japan, University of Okayama at Misasa (2003), 51p.
- [34] R.L. King, G.E. Bebout, T. Moriguti, E. Nakamura, Geochemistry of mélange formation: identifying contributions from mechanical and metasomatic mixing, *Geochim. Cosmochim. Acta* 67 (2003) A218.
- [35] V.J.M. Salters, A. Stracke, Composition of the depleted mantle, *Geochim. Geophys. Geosys.* 5 (2004) doi:10.1029/2003GC000597.
- [36] S. Weyer, C. Münker, K. Mezger, Nb/Ta, Zr/Hf, and REE in the depleted mantle: implications for the differentiation history of the crust–mantle system, *Earth Planet. Sci. Lett.* 205 (2003) 309–324.
- [37] R.K. Workman, S.R. Hart, Major and trace element composition of the depleted MORB mantle (DMM), *Earth Planet. Sci. Lett.* 231 (2005) 53–72.
- [38] T. Plank, Constraints from thorium/lanthanum on sediment recycling at subduction zones and the evolution of continents, *J. Petrol.* 46 (2005) 921–944.
- [39] S.-S. Sun, W.M. McDonough, Chemical and isotopic systematics of oceanic basalts: implications for mantle composition and processes, in: A.D. Saunders, M.J. Norry (Eds.), *Magma-tism in the ocean basins*, Geological Society of London, 1989, pp. 313–345.
- [40] M.T. McCulloch, Crust mantle recycling: inputs and outputs, in: S.R. Hart, L. Gülen (Eds.), *Crust/Mantle Recycling at Convergence Zones*, Kluwer, 1989, pp. 203–213.
- [41] T. Usui, E. Nakamura, K. Kobayashi, S. Maruyama, H. Helmstaedt, Fate of the subducted Farallon plate inferred from eclogite xenoliths in the Colorado Plateau, *Geology* 31 (2003) 589–592.
- [42] T. Usui, A geochemical study of the origin of eclogite xenoliths from the Colorado Plateau, southwestern United States: implications for the evolution of subducted oceanic crust [Ph.D. thesis]: Misasa, Tottori-ken, Japan, Okayama University at Misasa (2004), 171 p.
- [43] S.M. Peacock, Serpentinization and infiltration metasomatism in the Trinity peridotite, Klamath province, northern California: implications for subduction zones, *Contr. Mineral. Petrol.* 95 (1987) 55–70.
- [44] S.M. Peacock, Large-scale hydration of the lithosphere above subducting slabs, *Chem. Geol.* 108 (1993) 49–59.
- [45] C.E. Manning, Phase-equilibrium controls on SiO_2 metasomatism by aqueous fluid in subduction zones: reaction at constant pressure and temperature, *Int. Geol. Rev.* 37 (1995) 1074–1093.
- [46] C.E. Manning, Coupled reaction and flow in subduction zones: Si metasomatism of the mantle wedge, in: B. Jamtveit, B.W.D.

- Yardley (Eds.), *Fluid flow and transport in rocks*, Chapman and Hall, 1997, pp. 139–147.
- [47] R.L. King, M.J. Kohn, J.M. Eiler, Constraints on the petrologic structure of the subduction zone slab–mantle interface from Franciscan Complex exotic ultramafic blocks, *Geol. Soc. Amer. Bull.* 115 (2003) 1097–1109.
- [48] T. John, E.E. Scherer, K. Haase, V. Schenk, Trace element fractionation during fluid-induced eclogitization in a subducting slab: trace element and Lu–Hf–Sm–Nd isotope systematics, *Earth Planet. Sci. Lett.* 227 (2004) 441–456.
- [49] P.D. Noll, H.E. Newsom, W.P. Leeman, J. Ryan, The role of hydrothermal fluids in the production of subduction zone magmas: evidence from siderophile and chalcophile trace elements and boron, *Geochim. Cosmochim. Acta* 60 (1996) 587–611.
- [50] J. Yamamoto, S. Maruyama, C.D. Parkinson, I. Katayama, Geochemical characteristics of metabasites from the Kokchetav Massif: subduction zone metasomatism along an intermediate geotherm, in: C.D. Parkinson, I. Katayama, J.G. Liou, S. Maruyama (Eds.), *The diamond-bearing Kokchetav Massif, Kazakhstan*, Universal Academy Press, 2002, pp. 363–372.
- [51] F. Chalot-Prat, J. Ganne, A. Lombard, No significant element transfer from the oceanic plate to the mantle wedge during subduction and exhumation of the Tethys lithosphere (western Alps), *Lithos* 69 (2003) 69–103.
- [52] P. Philippot, J. Selverstone, Trace-element-rich brines in eclogitic veins: implications for fluid composition and transport during subduction, *Contr. Mineral. Petrol.* 106 (1991) 417–430.
- [53] D. Rumble, T.-F. Yui, The Qinglongshan oxygen and hydrogen isotope anomaly near Donghai in Jiangsu Province, China, *Geochim. Cosmochim. Acta* 62 (1998) 3307–3321.
- [54] A.C. Barnicoat, I. Cartwright, Focused fluid flow during subduction: oxygen isotope data from high-pressure ophiolites of the western Alps, *Earth Planet. Sci. Lett.* 132 (1995) 53–61.
- [55] J.A. Miller, I. Cartwright, I.S. Buick, A.C. Barnicoat, An O-isotope profile through the HP-LT Corsican ophiolite, France and its implications for fluid flow during subduction, *Chem. Geol.* 178 (2001) 43–69.
- [56] G.E. Bebout, The impact of subduction-zone metamorphism on mantle–ocean chemical cycling, *Chem. Geol.* 126 (1995) 191–218.
- [57] T. Elliot, T. Plank, A. Zindler, W. White, B. Bourdon, Element transport from slab to volcanic front at the Mariana arc, *J. Geophys. Res.* 102 (1997) 14991–15020.
- [58] T.P. Fischer, W.F. Giggenbach, Y. Sano, S.N. Williams, Fluxes and sources of volatiles discharged from Kudryavy, a subduction zone volcano, Kurile Islands, *Earth Planet. Sci. Lett.* 160 (1998) 81–96.
- [59] T.L. Grove, S.W. Parman, S.A. Bowring, R.C. Price, M.B. Barker, The role of an H₂O-rich component in the generation of basaltic andesites and andesites from the Mt. Shasta region, N. California, *Contr. Mineral. Petrol.* 142 (2002) 375–396.
- [60] B.R. Jicha, B.S. Singer, J.G. Brophy, J.H. Fournelle, C.M. Johnson, B.L. Beard, T.J. Lapen, N.J. Mahlen, Variable impact of the subducted slab on Aleutian island arc magma sources: evidence from Sr, Nd, Pb, and Hf isotopes and trace element abundances, *J. Petrol.* 45 (2004) 1845–1875.
- [61] R. George, S. Turner, J. Morris, T. Plank, C. Hawkesworth, J. Ryan, Pressure–temperature–time paths of sediment recycling beneath the Tonga–Kermadec arc, *Earth Planet. Sci. Lett.* 233 (2005) 195–211.
- [62] J.D. Woodhead, J.M. Hergt, J.P. Davidson, S.M. Eggins, Hafnium isotope evidence for ‘conservative’ element mobility during subduction zone processes, *Earth Planet. Sci. Lett.* 192 (2001) 331–346.
- [63] C. Münker, G. Wörner, G. Yogodzinski, T. Churikova, Behaviour of high field strength elements in subduction zones: constraints from Kamchatka–Aleutian arc lavas, *Earth Planet. Sci. Lett.* 224 (2004) 275–293.
- [64] C.E. Manning, The chemistry of subduction-zone fluids, *Earth Planet. Sci. Lett.* 223 (2004) 1–16.